

# Intratumorally CpG immunotherapy with carbon nanotubes inhibits local tumor growth and liver metastasis by suppressing the epithelial–mesenchymal transition of colon cancer cells

Hongyong Jin<sup>a</sup>, Sujie Gao<sup>b</sup>, Defeng Song<sup>a</sup>, Yiting Liu<sup>c</sup> and Xuebo Chen<sup>a</sup>

Colon cancer liver metastasis accounts for the major cause of death of colon cancer patients. Previous study reported a carbon nanotubes (CNT)-conjugated CpG complex (CNT-CpG), which displayed a significant antitumor effect in gliomas. However, whether CNT-CpG could limit colon tumor growth and suppress the colon cancer liver metastasis has not been evaluated. In this study, we report CNT enhances CpG uptake in mouse colon cancer cells. Results demonstrated only CpG with CNT conjugation showed significant activation of NF- $\kappa$ B signal. Moreover, intratumorally delivery of CNT-CpG successfully suppressed local xenograft tumor growth and liver metastasis. CNT-CpG treatments cured 75% of mice and inhibited local tumor growth, significantly prolonged survival outcomes and limited liver metastatic tumor nodules from colon cancer cells. Using human colon cancer cell line, HCT116, we observed significantly inhibitory effects of CNT-CpG on cell growth, invasion and migration. Importantly, CNT-CpG treatment blocked the epithelial to mesenchymal transition (EMT). We compared the mRNA levels of EMT markers of colon cancer cells without or with CNT-CpG treatment from in-vitro and in-vivo models. Consistent results demonstrated expression of epithelial marker,

E-cadherin was upregulated by CNT-CpG. In contrast, three mesenchymal markers, snail, fibronectin and vimentin were significantly suppressed by CNT-CpG treatment compared with control or free CpG. In summary, our data suggest CNT-CpG is an effective therapeutic approach against local colon tumor and their liver metastasis. This study presents the CNT-CpG complex as a promising therapeutic target for developing novel therapies against both local colon tumors and liver metastatic tumors. *Anti-Cancer Drugs* 32: 278–285 Copyright © 2020 The Author(s). Published by Wolters Kluwer Health, Inc..

*Anti-Cancer Drugs* 2021, 32:278–285

**Keywords:** carbon nanotube, colon cancer, carbon nanotubes-CpG, epithelial to mesenchymal transition, liver metastasis

<sup>a</sup>Department of General Surgery, <sup>b</sup>Department of Anesthesia, China-Japan Union Hospital of Jilin University, Changchun, Jilin Province and <sup>c</sup>Department of Radiology, Peking University School of Oncology, Beijing Cancer Hospital and Institute, Beijing, People's Republic of China

Correspondence to Xuebo Chen, Department of General Surgery, China-Japan Union Hospital of Jilin University, Changchun, Jilin Province 130033, People's Republic of China  
Tel: +86 15526891100; e-mail: chenxb@jlu.edu.cn

Received 29 March 2020 Revised form accepted 26 August 2020

## Introduction

Colon cancer is one of the most diagnosed and prevalent malignancies affecting both men and women worldwide [1]. Despite improvements in chemo- and radio-therapies and advances in surgical strategies, about one-third of colon cancer patients will develop metastatic disease and the prognosis for patients with metastatic disease is <13% [2,3]. Among the multiple organs where colon cancer cells migrate, liver metastasis accounts for the major cause of mortality of colon cancer patients because it is not suitable for surgery [3,4]. Thus, further investigation of critical molecular mechanisms is urgently needed to develop effective therapies that will improve the management of colon cancers with liver metastasis.

Malignant colorectal cancers have developed pathways to evade multiple immunosuppressive agents in immunotherapy [5,6]. Previous preclinical studies revealed the synthetic oligodeoxynucleotides containing unmethylated cytosine and guanine dinucleotides (CpG-ODN), a toll-like receptor 9 (TLR9) ligand have potent immunotherapeutic effects to enhance the anticancer activity of a variety of chemotherapies [7]. Clinically injections of high doses of CpG could trigger tumor suppression and induces long-term immunity against colon cancers [8]. However, studies showed an overdosage of the inflammatory response, intolerable toxicity and recurrence of tumors in patients hindered this approach [8–10]. To overcome this disadvantage, carbon nanotubes (CNTs)-conjugated CpG agent has been reported as an effective CpG carrier in gliomas [11]. CNTs are one kind of molecular-scale tubes of graphite carbon, which have unique mechanical properties that can be applied for specific drug delivery [11]. In addition, recent studies have demonstrated that soluble functionalized CNTs are nontoxic and most

This is an open-access article distributed under the terms of the Creative Commons Attribution-Non Commercial-No Derivatives License 4.0 (CCBY-NC-ND), where it is permissible to download and share the work provided it is properly cited. The work cannot be changed in any way or used commercially without permission from the journal.

of the CNTs will be metabolized and eliminated within 24 h of intravenous [12]. They showed that CNT-CpG can be taken up by gliomas both *in vitro* and *in vivo* and successfully triggered immune response and suppressed glioma tumor progressions [12]. However, the potentially antitumor effects of CNT-CpG in colorectal cancer have not been investigated.

Epithelial–mesenchymal transition (EMT) is the major cellular event carried out during both tumorigenesis and metastasis [13]. EMT is feathered by losing cell junctions, epithelial characteristics and cell polarity progress contributing to tumor metastasis and invasiveness [13,14]. Moreover, cancer cells that have undergone EMT are more malignant, displaying increased cancer feathers [14]. Studies revealed EMT programs are linked to the immune response of cancer cells: EMT could stimulate the production of proinflammatory factors; on the other way, local inflammation potentially induces EMT progresses in tumors [15]. Despite multiple studies pertaining to the effects of CNT-CpG in cancer immunotherapy, no substantial evidence has been established for the CNT-CpG-mediated tumor inflammation and EMT pathway.

Here, we used mouse colon cancer cells to establish a colon cancer xenograft and liver metastasis model. The *in-vitro* and *in-vivo* CpG uptake was enhanced by CNT-CpG. We examined the survival and liver metastatic tumor from mice with CNT-CpG immunotherapy. Interestingly, we found the EMT of colon cancer cells was effectively blocked by CNT-CpG. Our findings revealed that CpG therapy with a CNT delivery system could potentially be a promising therapeutic approach for colon tumors with liver metastasis.

## Materials and methods

### Cell lines and reagents

Human colon cancer cell line HCT116 and mouse colon cancer cell line CT26 were purchased from American Type Culture Collection and were cultured in RPMI1640 (Thermo Fisher Scientific, Inc., Carlsbad, California, USA) supplemented with 10% heat-inactivated endotoxin-free fetal bovine serum (FBS) (Thermo Fisher Scientific, Inc.), 100 units/mL penicillin and 100 µg/mL streptomycin (Thermo Fisher Scientific, Inc.) at 37°C in a humidified atmosphere with 5% CO<sub>2</sub>. Transforming growth factors (TGF)-β1 and 4',6-diamidino-2-phenylindole (DAPI) were purchased from Sigma-Aldrich (Shanghai, China) and diluted in dimethyl sulfoxide (DMSO). Thiolated CpG (5'-TGACTGTAACGTTTCGAGATGA-3') was constructed as described by previous reports [16]. The CNT-CpG construction and functionalization were performed according to previous reports [16]. The rabbit monoclonal antibody against SMAD2/3 was purchased from Cell Signaling Technology (Danvers, Massachusetts, USA).

### Measurement of cell growth

Cell growth curves were measured by 3-(4,5-dimethylthiazol-2-yl)-2,5-diphenyltetrazolium bromide (MTT)

assay. Cells (5 × 10<sup>3</sup> cells/well) were seeded into 96-well plates at 80% confluence. Cells were aspirated and washed with phosphate buffered saline (PBS), followed by adding MTT [3-(4,5-dimethylthiazol-2-yl)-2,5-diphenyltetrazolium bromide] solution at 37°C for 2 h. Samples in each well were incubated with 0.1 mL DMSO for 4 h at 37°C to solubilize the blue crystals. The optical density of formazan concentrations was determined at 570 nm by a Biotek Synergy H1 plate reader. Experiments were performed in triplicate and repeated three times.

### Scratch assay

Scratch assay was performed according to the previous description [17]. Briefly, cells were seeded into six-well plates at 2 × 10<sup>6</sup> cells/well for overnight at 37°C to allow cells to adhere completely. Then, a straight line was scratched using a P200 pipette tip. Plates were washed with PBS and replaced with a serum-free medium overnight. Cells were fixed with methional and the cell migration was observed under a microscope and pictures were taken. The distances between one side of the scratch and the other were labeled.

### Transwell invasion assay

Transwell assay was performed according to the previous description using a modified chamber (BD Falcon, San Jose, California, USA) [18]. Briefly, 7 × 10<sup>4</sup> cells were suspended and seeded onto the upper chambers. A medium containing 10% FBS was added to the lower chambers. After incubation for 24 h at 37°C in a humidified atmosphere with 5% CO<sub>2</sub>, cells were fixed with methional and stained with 1% crystal violet. The upper surfaces of the filters were wiped off with cotton swabs to remove nonmigrated cells. The migrated cells on the lower surface of the chambers were counted under a microscope. The experiments were performed in triplicate wells and repeated three times.

### CpG uptake assay

The *in-vitro* CpG uptake was detected by the methods as previously described [12]. CT26 cells were treated with Cy5.5-labeled CpG or CNT-CpG for 24 h. Cells were then fixed by 4% phosphate buffered saline/tween (PFA). The uptake of CpG was measured by detecting the immunofluorescence signals of Cy5.5-positive cells per field.

### Immunofluorescent staining

To detect the expression and translocation of SMAD2/3, HCT116 cells which were prepared in cover glass were fixed for 10 min by 4% PFA. The cell membrane was permeabilized with 0.5% Triton X-100 for 10 min. After washing with 0.1% Tween20 in PBS [phosphate buffered saline (PBST)], cells were incubated with blocking buffer (5% bovine serum albumin, and 0.1% Triton-X 100 in PBS) for 1 h at room temperature. The primary antibodies against SMAD2/3 (1:200 dilution, Cell Signaling, Danvers, Massachusetts, USA), were incubated with fixed cells at 4°C

overnight with gentle agitation. After washing completely with PBST, Alexa 594 conjugated goat antirabbit (1:5000 dilution, Life Technologies, Carlsbad, California) antibodies were added into a blocking buffer for 1 h at room temperature in a dark chamber. Cell nuclei were stained with DAPI (Vector Laboratories, Inc.; Burlingame, California, USA) for 2 min at room temperature. Fluorescence images were taken by the Carl Zeiss Confocal Imaging System (LSM 780; Carl Zeiss, Jena, Germany).

#### **In-vitro NF- $\kappa$ B assay**

The detection of NF- $\kappa$ B activity was performed according to previous reports [12]. Briefly, RAW MP cells (RAW-Blue) were stably transfected with a reporter construct which was under the control of a promoter inducible by NF- $\kappa$ B. Upon free CpG or CNT-CpG stimulation, RAW-Blue cells will induce the activation of NF- $\kappa$ B, the activity of which will be subsequently detected by the reporter signaling. Experiments were performed in triplicate and repeated three times. Results were normalized by cell number of each well.

#### **RNA isolation and quantitative real-time PCR**

Total RNA was isolated by Trizol (Thermo Fisher Scientific, Inc.) method according to the manufacturer's instruction. Concentrations of RNA samples were assessed using the NanoDrop spectrophotometer (Thermo Fisher Scientific, Inc.) followed by double DNase treatment and purification using the Qiagen RNeasy Clean-up protocol. cDNA was synthesized by the FastQuant cDNA First-Strand Synthesis kit (Tiangen Biotech, Co., Ltd., Beijing, China). Real-time PCR was performed using the FastStart Universal SYBR Green Master Mix (Thermo Fisher Scientific, Inc.) according to the manufacturer's instructions. The reaction cycling conditions were performed as follows: 1 cycle at 95°C for 15 min, then 40 cycles at 95°C for 10 s and at 60°C for 60 s. Glyceraldehyde 3-phosphate dehydrogenase (GAPDH) was used as an internal control. Primers for quantitative real-time PCR (qRT-PCR) in this study were: E-cadherin, forward: 5'-GTCACCTGACACCAACGATAATCCT-3' and reverse: 5'-TTTCAGTGTGGTGATACGACGTTA-3'; Snail, forward: 5'-ACCACTATGCCGCGCTCTT-3' and reverse: 5'-GGTCGTAGGGCTGCTGGAA-3'; fibronectin, forward: 5'-CCCACCGTCTCAACATGCTTAG-3' and reverse: 5'-CTCGGCTTCCTCCATAACAAGTAC-3'; vimentin, forward: 5'-TCTACGAGGAGGAGATGCGG-3' and reverse: 5'-GGTCAAGACGTGCCAGAGAC-3'; GAPDH, forward: 5'-ACCACAGTCCATGCCATCAC-3' and reverse: 5'-TCCACCCTGTTGCTGTA-3'. The relative expressions of EMT marker mRNAs were calculated using the  $2^{-\Delta\Delta Ct}$  method. All reactions were performed in duplicate and repeated three times.

#### **Immunohistochemistry**

The staining of E-cadherin and vimentin proteins from mice tumors were performed according to previous reports [18].

#### **Western blot**

Cells were collected and lysates were added 4°C radioimmunoprecipitation assay lysis buffer (Thermo Fisher Scientific, Inc.) including 1X protease inhibitor cocktail (Thermo Fisher Scientific, Inc.). After 15 min incubation on ice, total proteins were extracted by centrifuging at 10000g for 15 min at 4°C. Protein concentration was quantified using a bicinchoninic acid assay kit (Thermo Scientific, Waltham, Massachusetts, USA) according to the manufacturer's instructions. Forty microgram samples were separated onto 10 or 12% SDS-PAGE gel and electro-transferred onto nitrocellulose membranes (Biorad, Shanghai, China). Membranes were blocked by 5% non-fat milk in tris buffered saline/tween (TBST) for 30 min at room temperature, followed by incubation of primary antibodies at 1:1000 at 4°C for overnight. After complete washing by TBST, membranes were incubated with secondary antibody for 1 h at room temperature. Protein bands were specifically detected by Enhanced Chemiluminescent horseradish peroxidase Substrate solution and the Image Quant LAS 4000 Imaging System (Millipore, Shanghai, China). GAPDH was a loading control. Experiments were repeated three times.

#### **In-vivo tumor xenograft and liver metastasis analysis**

Totally 38-week-old C57BL/6 mice were used in this study. Mice were kept on a regular 12/12 h light-dark cycle cages with access to food and water. Experimental mice were injected subcutaneously with CT26 mouse colon cancer cells ( $1 \times 10^7$ ) to establish xenograft models. Tumor progress was monitored every 3 days until tumors reached a size of greater than 100 mm<sup>3</sup>. Mice from each xenograft group were then randomly divided into three groups (10 mice per group) and treated as follows: PBS control; free CpG alone (40 mg/kg intraperitoneal, two times per week) or CNT-CpG (500 mg/kg, intraperitoneal, two times per week). Mice mortality was monitored daily. The sizes of the tumors were measured every 3 days. After 80 days the mice were euthanized, and the xenograft tumor tissues were dissected and immediately frozen in liquid nitrogen and stored at -80°C for downstream analysis. For the liver metastasis analysis, the mice were sacrificed, and the livers were resected. The nodule number of each liver was counted as previous reports [19]. Experiment protocols were reviewed and approved by an institutional review committee from Institutional Animal Care and Use Committee of the China-Japan Union Hospital of Jilin University. Experiments were carried out in accordance with the European Communities Council Directive of 24 November 1986 (86/609/EEC).

#### **Statistical analysis**

Statistical analysis was performed using GraphPad Prism 6.0 (GraphPad Software, La Jolla, California, USA). Experiments were repeated three times. Data were presented as mean  $\pm$  SEM. Results compared between two groups were analyzed by paired Student *t*-tests. Multiple group comparisons were analyzed by one-way analysis

of variance. A  $P$  value  $<0.05$  was considered statistically significant.

## Results

### Carbon nanotubes enhance CpG uptake *in vitro*

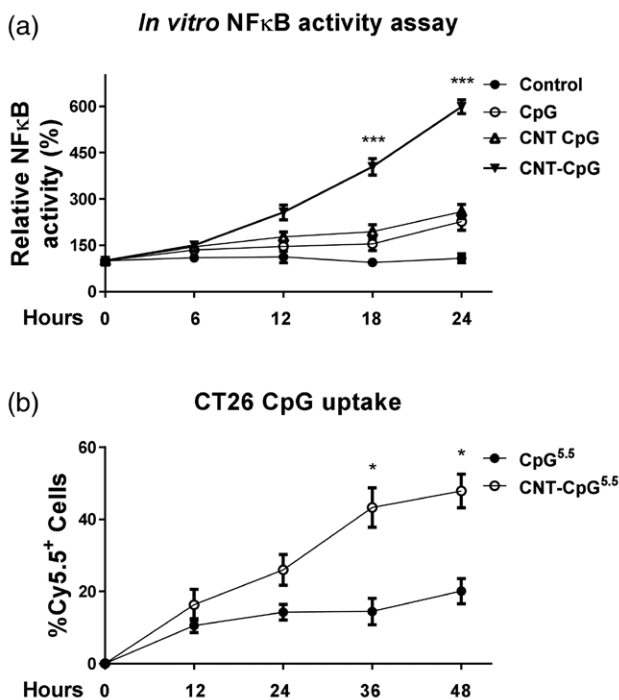
To assess whether the CNTs-conjugated CpG was more effective than free CpG on colon cancer cells progresses, we firstly examined the CNT-CpG activity using an *in-vitro* NF- $\kappa$ B assay prior to animal studies. RAW-Blue cells were incubated with control, soluble CpG alone, CNT plus CpG or CNT conjugated CpG (CNT-CpG). The NF- $\kappa$ B activity was measured by an alkaline phosphatase activity assay. Results demonstrated only CpG with CNT conjugation showed significant activation of NF- $\kappa$ B signal (Fig. 1a). In this study, we picked CNT-CpG preparations that the NF- $\kappa$ B activity was increased more than two-fold over an equivalent dose of free CpG for downstream *in-vivo* experiments. We next evaluated *in-vitro* loading capacity of CNT-CpG in mouse colon cancer cell line, CT26 which were incubated with CNT bound to Cy5.5-labeled CpG (CNT-CpG5.5) or free

CpG5.5. The CpG uptake capacity of CT26 cells was significantly enhanced by CNT conjugation (Fig. 1b). These results demonstrated that the intracellular CpG delivery could be increased with CNTs.

### Intratumorally delivery of carbon nanotubes-CpG suppresses local xenograft tumor growth and liver metastasis

To evaluate the *in-vivo* antitumor effects of CNT-CpG immunotherapy, an *in-vivo* colon cancer cells xenograft and liver metastasis model was established. CT26 cells were injected into mice and when the tumor was established, mice were given an injection of PBS (control), free CpG or CpG conjugated with CNT at an effective dosage to eradicate gliomas (i.e. 5 mg). Expectedly, results showed a low-dose injection of free CpG had limit antitumor effects. The mice with control or free CpG alone treatments had low survival rates and enlarged local tumor sizes (Fig. 2a–c). In contrast, CNT-CpG treatments cured 75% of mice and inhibited tumor growth, significantly prolonged survival outcome (Fig. 2a–c). Since colon cancer liver metastasis is one of the main obstacles in colon cancer treatment [13]. We next assessed the effects of CNT-CpG on metastasis of colon cancer cells. First, we established a liver metastasis platform using mouse colorectal cancer cell line, CT26. We detected the capability of CT26 cells to form hepatic metastasis from the colorectal cancer xenograft mouse model and results showed the significant capability of forming hepatic metastasis (data not shown). Upon mice sacrifice and examination at 42 days postinoculation, mice with established liver metastases under the CNT-CpG treatment showed significantly reduced metastatic nodules compared with PBS and free CpG alone treatments (Fig. 2d and e). In summary, the above results demonstrated CNT-CpG treatments effectively inhibited local colon tumor growth and liver metastasis.

Fig. 1

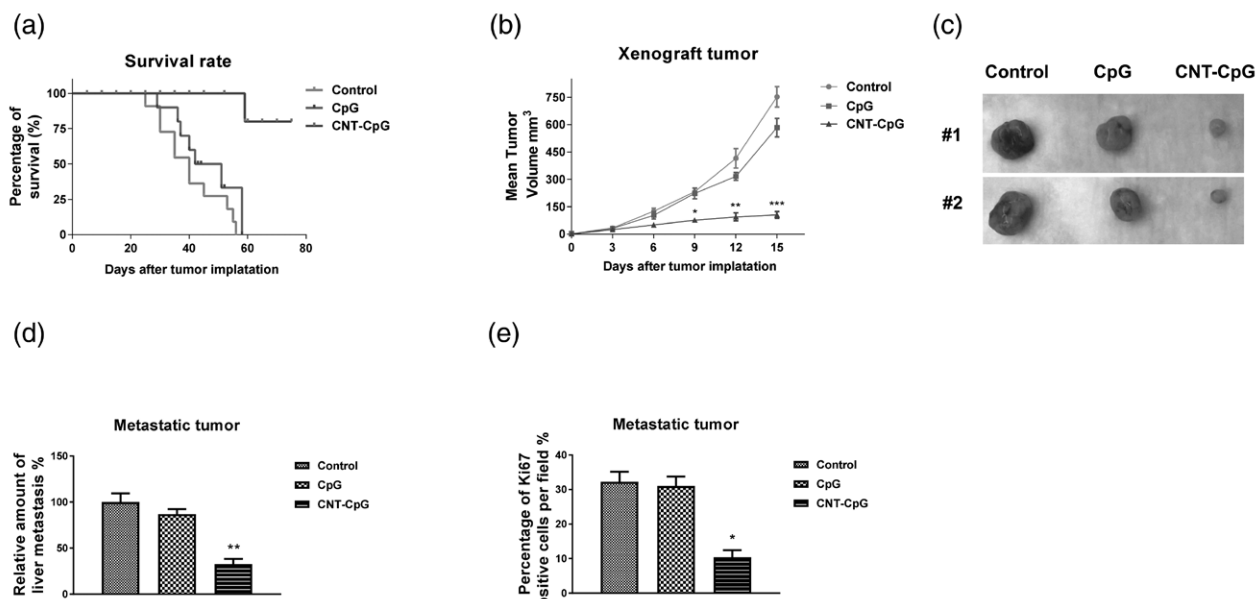


CNTs enhance CpG uptake *in vitro*. (a) *In-vitro* CNT-CpG activity was measured by an *in-vitro* NF- $\kappa$ B assay. RAW-Blue cells were incubated with CNT at 25  $\mu$ g/mL, free CpG at 1 mM, or CNT-CpG (25  $\mu$ g/mL CNT conjugated with 1 mM CpG) for 24 h. The NF- $\kappa$ B activity was examined by measuring alkaline phosphatase activity. (b) CT26 cells were incubated with CpG5.5 or CNT-CpG5.5 at 0, 12, 24, 36 or 48 h. Percentages of the Cy5.5 + cells were counted under fluorescence microscope. Results demonstrated that CNTs enhance CpG uptake in CT26 cells. Data are representative of three separate experiments. \* $P < 0.05$ ; \*\*\* $P < 0.001$ . CNT, carbon nanotubes.

### In-vitro inhibitory effects of carbon nanotube-CpG on cell growth, invasion and migration of colon cancer cells

We next evaluated the underlying mechanisms for the CNT-CpG-mediated liver metastasis. Using an *in-vitro* model, both human and mouse colorectal cancer cell lines, HCT116 and CT26 showed significantly inhibited growth rates by CNT-CpG treatments compared with PBS or free CpG treatment (Fig. 3a and b). To further evaluate the influence of CNT-CpG on colon cancer cell metastasis, wound-healing, and invasion assays were performed. As we expected, the lower motility capacities in HCT116 and CT26 cells with CNT-CpG treatment were observed compared with control or free CpG treatment which showed a closer gap between the wound edges (Fig. 3c). Consistently, the invasive behaviors of HCT116 and CT26 cells were significantly decreased with the treatment of CNT-CpG from transwell assay (Fig. 3d and

Fig. 2



CNT-CpG abrogates growth of colon tumor and liver metastasis following intratumoral injection. (a) Mice bearing CT26 colon tumors were treated with intratumoral injections of saline or free CpG at 1 mM or CNT-CpG (25  $\mu$ g/mL CNT conjugated with 1 mM CpG) at 7 and 14 days after initial tumor implantation. Mice survival rates were examined each day and recorded. (b) Tumor sizes from mice with the above treatments were measurements with calipers and calculated every 3 days. (c) Two representative tumors from the above-treated mice were shown. (d) Amounts and (e) cancer cell numbers of liver metastatic tumor nodules from the above mice with same treatments were measured. Columns, mean of three independent experiments; bars, SE. \* $P < 0.05$ ; \*\* $P < 0.01$ . CNT, carbon nanotube.

e). These in-vitro results indicate that CNT-CpG treatment could effectively suppress the metastasis ability of colon cancer cells.

### Carbon nanotube-CpG treatment blocks the epithelial-mesenchymal transition of colon cancer cells

It is widely known that cancer cells that undergone EMT are more aggressive and invasive [14]. To investigate the molecular mechanisms for the CNT-CpG-inhibited colon cancer cell migration, we examined the EMT phenotype on colon cancer cells without or with CNT-CpG treatment. Interestingly, we observed an obvious morphological change on HCT116 cells from polarized epithelial cells that are connected via adhesion to mesenchymal with TGF- $\beta$  induction [14], while this morphological change was reversed by CNT-CpG but not free CpG treatment (Fig. 4a). In addition, the TGF- $\beta$ -induced translocation of SMAD2 and SMAD3 into nuclei, an EMT marker of cancer cells, was significantly blocked by CNT-CpG treatment compared with control (Fig. 4b). Consistently, the expression of epithelial marker, E-cadherin was upregulated by CNT-CpG (Fig. 4c and d). Meanwhile, three mesenchymal markers, snail, fibronectin and vimentin were significantly suppressed by CNT-CpG treatment compared with control or free CpG (Fig. 4c and d). The above results revealed CNT-CpG could suppress the EMT of colon cancer cells.

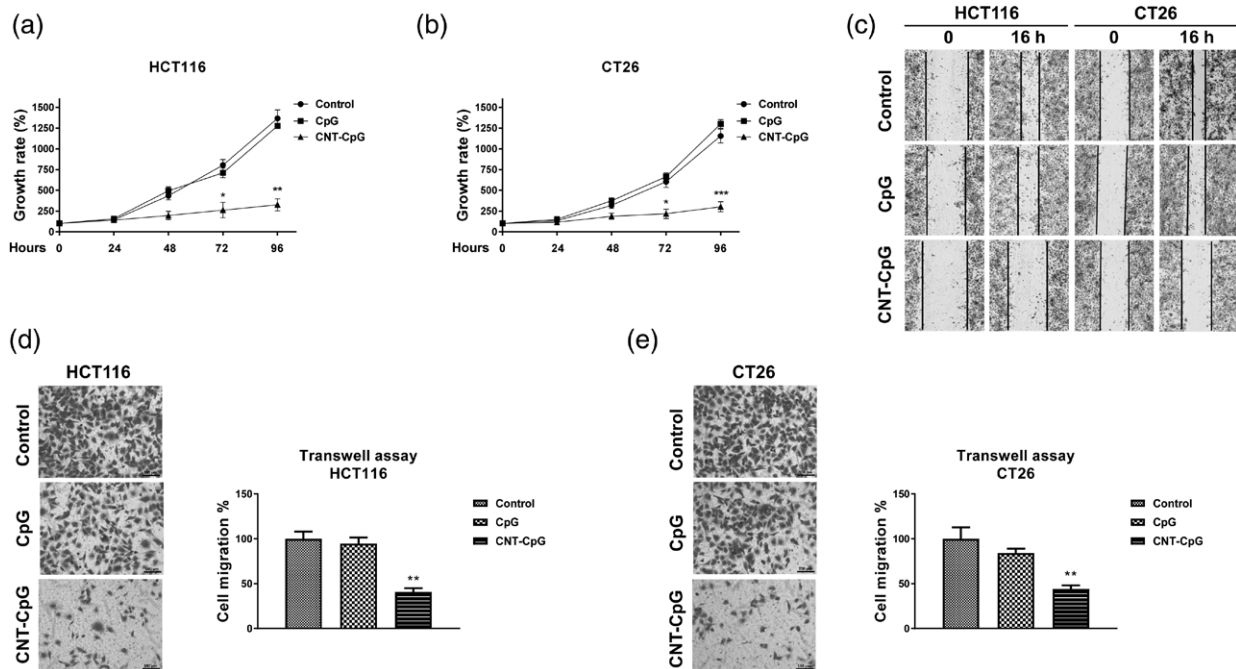
### In-vivo inhibition of epithelial-mesenchymal transition of local xenograft tumor by carbon nanotube-CpG treatment

To verify the above in-vitro results, we further examined the mRNA expressions from local xenograft tumors with control, free CpG or CNT-CpG treatment. Consistent with results from colon cancer cells, the epithelial marker, E-cadherin was obviously induced in mice tumors receiving CNT-CpG treatment (Fig. 5a and c). On the contrast, CNT-CpG treated mice tumors displayed significantly downregulated expressions of mesenchymal marker, vimentin (Fig. 5b and c). Taking together, our in-vitro and in-vivo results, therefore, suggest CNT-CpG is an effective approach against liver metastasis originating from colorectal tumors.

### Discussion

Recent studies reported that systemic administration of synthetic oligodeoxynucleotides containing unmethylated CpG motifs (CpG-ODN) worked as effective immune stimulators to activate innate immunity through TLR [20]. Thus, CpG-ODN or peritumoral administration of CpG-ODN is a potential therapeutic approach for inhibiting tumor growth and metastasis [21]. Although CpG could enhance its proinflammatory effect, high-dosage application of CpG could further exacerbate tumor environment and result in toxicity by

Fig. 3



CNT-CpG treatments suppress cell growth, migration and invasion of colon cancer cells. (a) HCT116 and (b) CT26 cells were treated with control, free CpG or CNT-CpG for 24 h. The cell growth rates were measured by MTT assay. (c) HCT116 and CT26 cells were treated with control, free CpG or CNT-CpG for 24 h. Cells were seeded in six-well plated for overnight, motility of cells was examined using a wound-healing migration assay. (d) HCT116 and (e) CT26 cells were treated with control, free CpG or CNT-CpG for 24 h. The cells' invasive capacities were detected using the BD BioCoat Matrigel Invasion Chamber. After 24 h, cells on the reverse side were counted as migrated cells. Experiments were performed in triplicate. Columns, mean of three independent experiments; bars, SE. \* $P < 0.05$ ; \*\* $P < 0.01$ . CNT, carbon nanotube; MTT, 3-(4,5-dimethylthiazol-2-yl)-2,5-diphenyltetrazolium bromide.

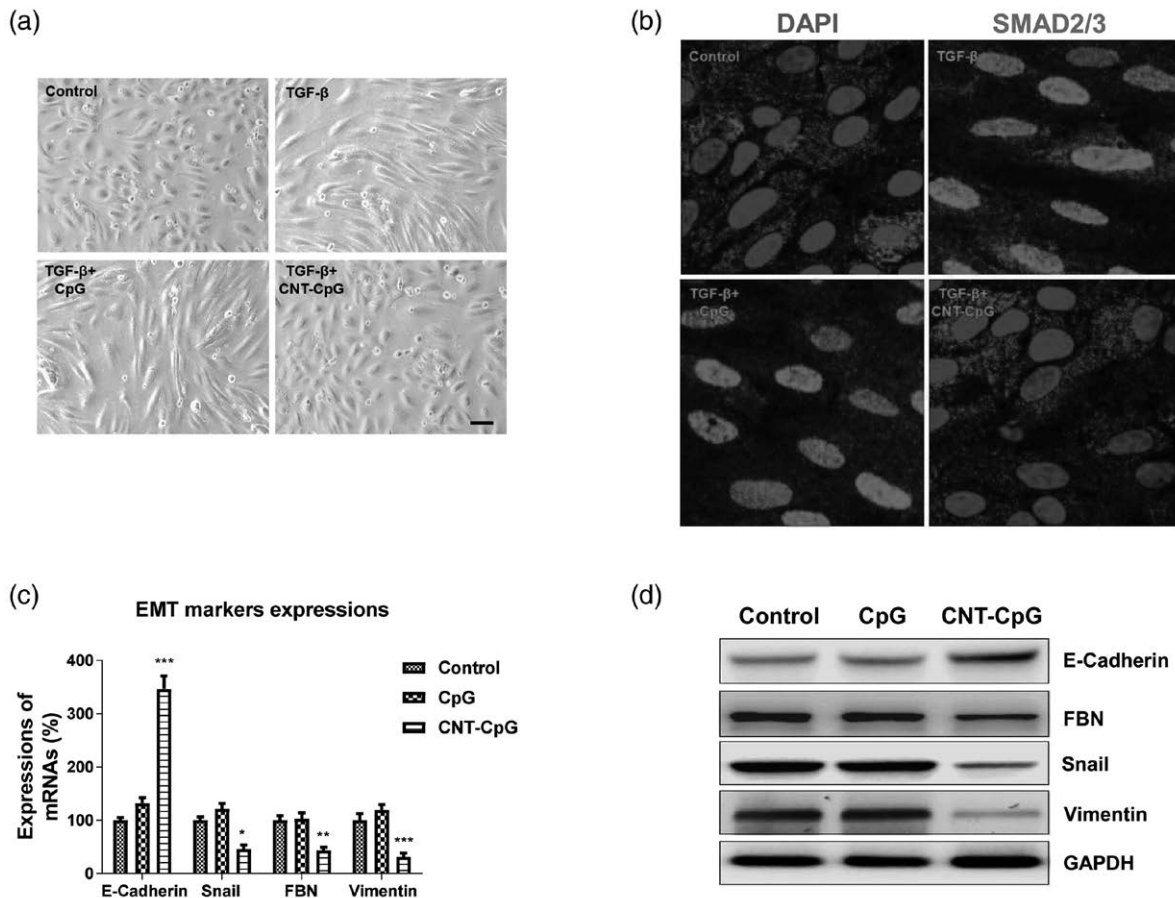
activating alternative TLR9-independent pathways [8–10]. Repeated low-dose CpG injection can augment the proinflammatory CpG response [8–10]. On the basis of our previous reports, here we demonstrate that functionalized CNTs enhanced CpG uptake by colon cancer cells, indicating the effective CNT-CpG deliver system was an immunotherapy approach. Although the application of CNT-CpG has been examined in melanoma before [12], our study firstly demonstrated the anti-cancer efficacy of CNT-CpG complexes in colon cancer from both *in vitro* and *in vivo*. Our data indicate that improved delivery of CpG into the colon cancer-bearing xenograft tumor by CNTs successfully inhibited local tumor growth and increased survival rates of CNT-CpG treated mice.

It was known that liver metastasis, which accounts for the major cause of mortality of colon cancer patients is the most commonly metastasized organ in colon cancer [14]. Synchronous liver metastasis can be found in up to 25% of colon cancer patients [4]. Thus, better understanding the molecular mechanisms of colorectal cancer liver metastasis (CCLM) and develop new therapeutic methods are urgent for clinical administration of CCLM. Previous reports demonstrated intracerebral injection of CNT-CpG could successfully suppress metastatic brain tumors

[11]. However, little is known about whether CNT-CpG affects the metastasized liver tumors from the primary tumor site. In this study, we observed that CNT-CpG, in contrast to free CpG, which only had a modest inhibitory effect on local and liver metastatic tumor growth, significantly abrogated the liver metastasis from colon tumors, presenting the CNT-CpG delivery system has potential advantages over other nanomaterials and more clinical applications against multiple tumor metastasis.

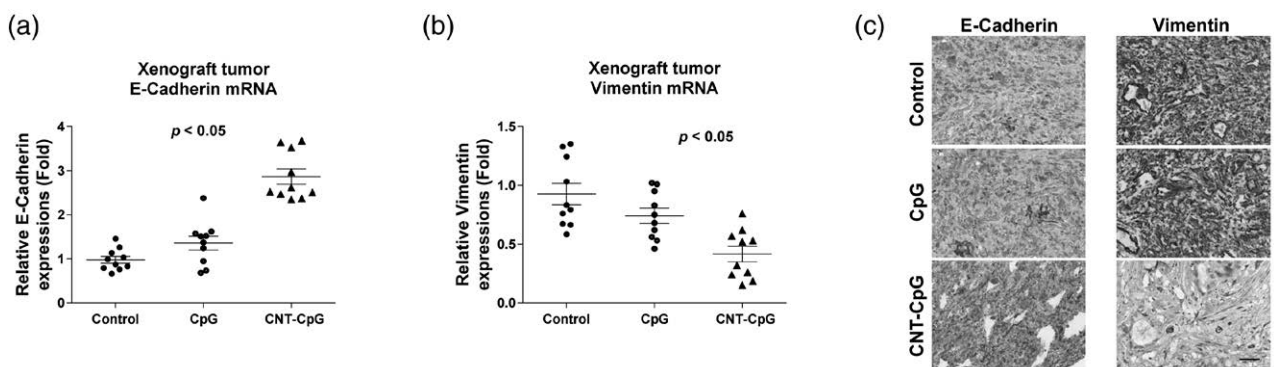
The EMT renders cancer cells more aggressive, accompanying with increased invasiveness and resistance to apoptosis [13]. Interestingly, increasing evidence have emphasized the association between cancer cells EMT and inflammation. Inflammatory mediators such as oxidative stress or hypoxia could promote the EMT-like features in cancer cells [15]. On the other way, malignant cancer cells could produce elevated amount of proinflammatory mediators, such as cytokines [15]. In this study, we described the connections between EMT signaling pathways and the CNT-CpG stimulated inflammation of colon tumors from in-vitro and in-vivo models. CNT-CpG treatment significantly blocked the TGF- $\beta$  induced EMT of colon cancer cells. We found the nuclear translocation of transcription factor SMAD2/3 was decreased by

Fig. 4



CNT-CpG treatments blocked the TGF- $\beta$ -induced EMT of colon cancer cells. (a) HCT116 cells were treated with control, TGF- $\beta$  (10 ng/mL), TGF- $\beta$  (10 ng/mL) plus free CpG or TGF- $\beta$  (10 ng/mL) plus CNT-CpG for 24 h. Morphological changes were observed and recorded under microscope. (b) The above treated HCT116 cells were fixed and stained by DAPI and SMAD2/3 (Cy3). Expressions and localization of SMAD2/3 were observed and analyzed under a fluorescence microscope. mRNA and protein expressions of EMT marker genes were detected by (c) qRT-PCR and (d) western blot from HCT116 cells with the same treatments. GAPDH was an internal control. Experiments were performed in triplicate. Columns, mean of three independent experiments; bars, SE. \* $P < 0.05$ ; \*\* $P < 0.01$ . CNT, carbon nanotube; DAPI, 4',6-diamidino-2-phenylindole; EMT, epithelial-mesenchymal transition; GAPDH, glyceraldehyde 3-phosphate dehydrogenase; TGF, transforming growth factors.

Fig. 5



CNT-CpG blocks EMT of colon cancer cells *in vivo*. (a) Expressions of epithelial marker, E-cadherin and (b) mesenchymal marker, vimentin were detected by qRT-PCR from xenograft tumors of mice with the intratumoral injection of saline, free CpG alone or CNT-CpG. GAPDH was an internal control. (c) Protein expressions of E-cadherin and vimentin were detected by immunohistochemistry staining from above xenograft tumors. Experiments were performed in triplicate. Columns, mean of three independent experiments; bars, SE.  $P < 0.05$ . CNT, carbon nanotube; EMT, epithelial-mesenchymal transition.

CNT-CpG treatment. In addition, expressions of EMT markers snail, vimentin and fibronectin were significantly downregulated by CNT-CpG treatment. Consistently, from the colon cancer xenograft mice tumors, we detected epithelial cell marker, E-cadherin was upregulated and the mesenchymal cell marker, vimentin was significantly suppressed by CNT-CpG treatments.

### Conclusion

In summary, our data demonstrated CNT-CpG is an effective therapeutic approach against not only local colon tumor growth but their liver metastatic tumors. Using in-vitro and in-vivo models, we illustrated the EMT pathway was significantly blocked by CNT-CpG treatment. This study presents the CNT-CpG complex as a promising therapeutic target to develop novel therapies against both local colon tumors and liver metastatic tumors.

### Acknowledgements

The authors would sincerely thank all the doctors, research faculties and staff from the Department of General Surgery, China-Japan Union Hospital of Jilin University, Changchun, Jilin. The authors also thank the reviewers and editors for critically and thoughtful comments for this article.

This work was supported by the Natural Science Foundation of Science and Technology Development Plan in Jilin Province, China (No. 20180101303JC).

X.C. and S.G. designed the study. H.J., S.G., D.S. and Y.L. carried out the experiments. H.J., S.G., D.S. and Y.L. analyzed and interpreted the results. S.G. and X.C. wrote the manuscript. H.J. and X.C. performed the statistical analysis.

### Conflicts of interest

There are no conflicts of interest.

### References

- Meyers BM, Cosby R, Queresby F, Jonker D. Adjuvant chemotherapy for stage II and III colon cancer following complete resection: a cancer care Ontario systematic review. *Clin Oncol (R Coll Radiol)* 2017; **29**:459–465.
- Lee JJ, Chu E. The adjuvant treatment of stage III colon cancer: might less Be more? *Oncology (Williston Park)* 2018; **32**:437–42, 444.
- Hanna K, Zeeshan M, Hamidi M, Pandit V, Omesiete P, Cruz A, *et al.* Colon cancer in the young: contributing factors and short-term surgical outcomes. *Int J Colorectal Dis* 2019; **34**:1879–1885.
- Riihimäki M, Hemminki A, Sundquist J, Hemminki K. Patterns of metastasis in colon and rectal cancer. *Sci Rep* 2016; **6**:29765.
- Terzić J, Grivennikov S, Karin E, Karin M. Inflammation and colon cancer. *Gastroenterology* 2010; **138**:2101–2114.e5.
- Zhou R, Zhang J, Zeng D, Sun H, Rong X, Shi M, *et al.* Immune cell infiltration as a biomarker for the diagnosis and prognosis of stage I–III colon cancer. *Cancer Immunol Immunother* 2019; **68**:433–442.
- Hanagata N. CpG oligodeoxynucleotide nanomedicines for the prophylaxis or treatment of cancers, infectious diseases, and allergies. *Int J Nanomedicine* 2017; **12**:515–531.
- Carpentier A, Laigle-Donadey F, Zohar S, Capelle L, Behin A, Tibi A, *et al.* Phase 1 trial of a CpG oligodeoxynucleotide for patients with recurrent glioblastoma. *Neuro Oncol* 2006; **8**:60–66.
- Weber JS, Zarour H, Redman B, Trefzer U, O'Day S, van den Eertwegh AJ, *et al.* Randomized phase 2/3 trial of CpG oligodeoxynucleotide PF-3512676 alone or with dacarbazine for patients with unresectable stage III and IV melanoma. *Cancer* 2009; **115**:3944–3954.
- Carpentier A, Metellus P, Ursu R, Zohar S, Lafitte F, Barrié M, *et al.* Intracerebral administration of CpG oligonucleotide for patients with recurrent glioblastoma: a phase II study. *Neuro Oncol* 2010; **12**:401–408.
- Zhao D, Alizadeh D, Zhang L, Liu W, Farrukh O, Manuel E, *et al.* Carbon nanotubes enhance CpG uptake and potentiate antitumor immunity. *Clin Cancer Res* 2011; **17**:771–782.
- Fan H, Zhang I, Chen X, Zhang L, Wang H, Da Fonseca A, *et al.* Intracerebral CpG immunotherapy with carbon nanotubes abrogates growth of subcutaneous melanomas in mice. *Clin Cancer Res* 2012; **18**:5628–5638.
- San Juan BP, Garcia-Leon MJ, Rangel L, Goetz JG, Chaffer CL. The complexities of metastasis. *Cancers (Basel)*. 2019; **11**:1575.
- Zhang Y, Weinberg RA. Epithelial-to-mesenchymal transition in cancer: complexity and opportunities. *Front Med* 2018; **12**:361–373.
- Suarez-Carmona M, Lesage J, Cataldo D, Gilles C. EMT and inflammation: inseparable actors of cancer progression. *Mol Oncol* 2017; **11**:805–823.
- Liu Z, Tabakman SM, Chen Z, Dai H. Preparation of carbon nanotube bioconjugates for biomedical applications. *Nat Protoc* 2009; **4**:1372–1382.
- Chen Z, Wang Y, Liu W, Zhao G, Lee S, Balogh A, *et al.* Doxycycline inducible Krüppel-like factor 4 lentiviral vector mediates mesenchymal to epithelial transition in ovarian cancer cells. *PLoS One* 2014; **9**:e105331.
- Tang B, Liang W, Liao Y, Li Z, Wang Y, Yan C. PEA15 promotes liver metastasis of colorectal cancer by upregulating the ERK/MAPK signaling pathway. *Oncol Rep* 2019; **41**:43–56.
- Banerjee D, Hernandez SL, Garcia A, Kangsamaksin T, Sbiroli E, Andrews J, *et al.* Notch suppresses angiogenesis and progression of hepatic metastases. *Cancer Res* 2015; **75**:1592–1602.
- Nie Y, He J, Shirota H, Trivett AL, Yang D, Klinman DM, *et al.* Blockade of TNFR2 signaling enhances the immunotherapeutic effect of CpG ODN in a mouse model of colon cancer. *Sci Signal* 2018; **11**:eaan0790.
- Olbert PJ, Schrader AJ, Simon C, Dalpke A, Barth P, Hofmann R, Hegele A. *In vitro* and *in vivo* effects of CpG-oligodeoxynucleotides (CpG-ODN) on murine transitional cell carcinoma and on the native murine urinary bladder wall. *Anticancer Res* 2009; **29**:2067–2076.